

# Mechanical analysis of MBHDP301b assembly and test

Carmen Abad on behalf 11Tesla team

Diego Perini, Ruth Diaz Vez, Cedric Garion, Marco Morrone,  
Francois-Olivier Pincot, Frederic Savary, Attilio Milanese, Susana  
Izquierdo Bermudez, Nicolas Bourcey, Nicholas Lusa, Sebastien  
Luzieux, Michael Guinchard, Sylvain Mugnier, Franco Julio  
Mangiarotti, Gerard Willering, Jerome Freuvrier, Filip Kosowski,  
Jean-Luc Guyon, Patrick Viret

Meeting category:

<https://indico.cern.ch/category/5095/>

Meeting:

<https://indico.cern.ch/event/1430746/>

# Content

## 1. Introduction

- Context
- Magnet new mechanical features

## 2. Magnet fabrication

- Mechanical instrumentation
- Coils
- Shimming plan
- End cage

## 3. Cold test results

## 4. Mechanical measurements

- Some words
- Collar nose stress
- Magnet end plate bullets
- End cage rods

## 5. Conclusion

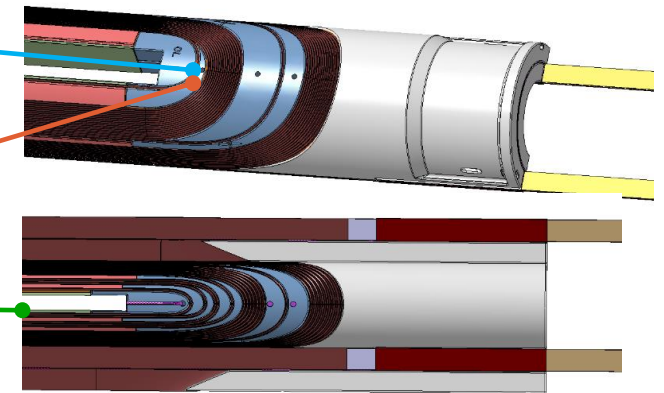
## 6. References

# 1. Introduction

# Context

After the test of four 11T series magnets (S1, S2, S3, S4), three of them showed performance degradation and the quenches were localized primarily in the coil heads. These results led to the decision not to install the 11T magnets during Long Shutdown 2 (LS2) and to reassess the next steps. Subsequent research, including tomography, metallographic analysis, and comparison with a 3D FEA analysis [1] revealed high stress areas in the coil ends, that correspond to the quench localizations in S2 and S4. Two types of issues were identified, internal to the coils and external to the coils. The internal are outside of the scope of this study because they can't be addressed without manufacturing new coils. The external identified are:

1. High stressed areas and stress singularities **after collaring** in the coil outer layer's first turn.
2. High stressed areas and stress singularities **after cool-down** in the coil outer layer's first turn.
3. High peak stresses **during powering** in the coil inner layer turns.
4. **Non-optimal coil end support** for the electromagnetic axial force difference in between the blocks.
5. **Non-optimal axial loading**. S2 & S3 cold masses had a loosened and deformed axial loading screw (bullet).



# Magnet new mechanical features

To assess the high stressed areas, new mechanical features are installed in a double aperture hybrid prototype.

## Mitigation measures 1 (Aperture 1, SP301)

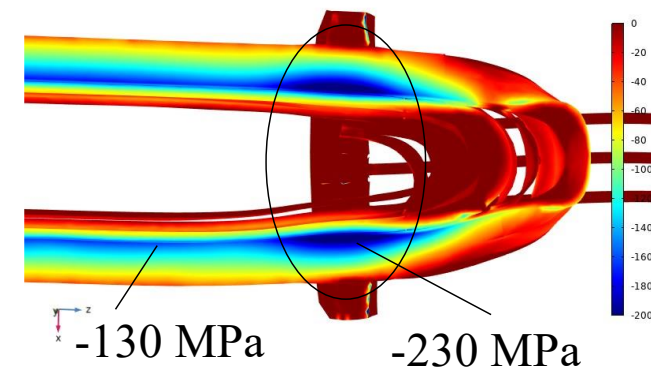
- New shimming plan with excess reduction in the ends.
- Pole material change from Titanium to austenitic Stainless Steel.
- With these two new features a reduction of the high peak stresses during powering is observed in the 3D FEA [1].

## Mitigation measures 2 (Aperture 2, SP302)

### Mitigation measures 1 + end cage system

Objective: compact the head coil blocks during powering and improve the axial loading.

Drawback: azimuthal stress in coil inner layer increase at the position of the end cage



Courtesy of M. Morrone C. Garion

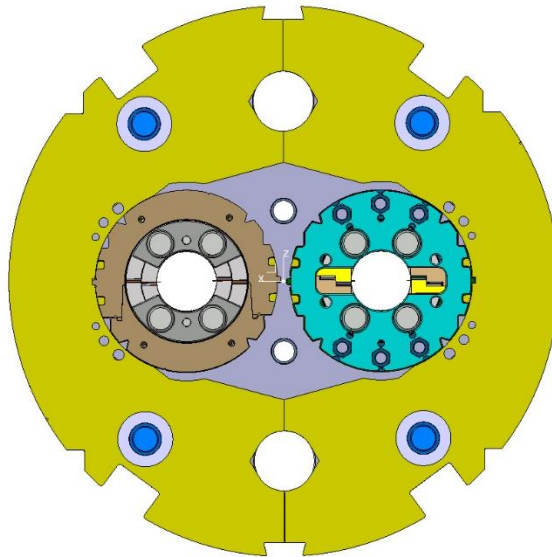
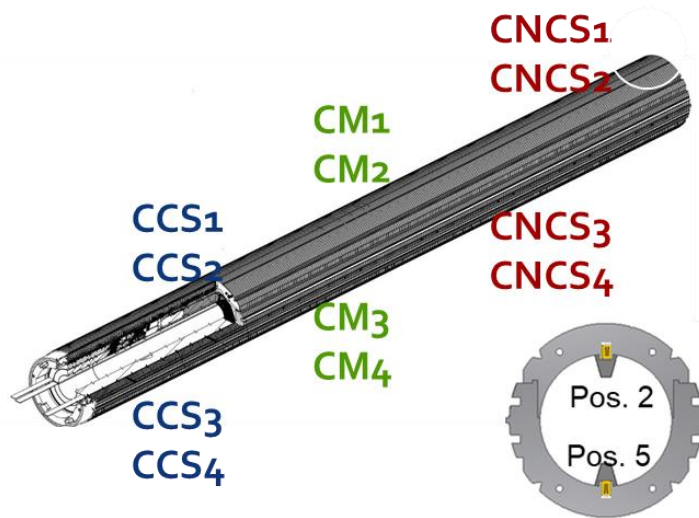
In previous models, the peak stresses on the mid plane has been found as one of the limitation for the coil performance [2].

# 2. Magnet fabrication

# Mechanical instrumentation

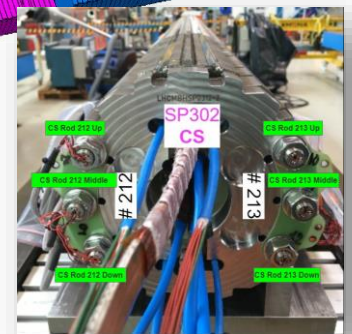
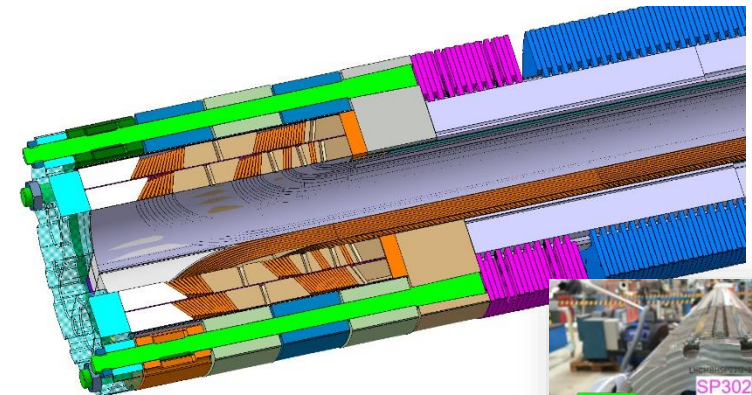
## SP301

- 12 instrumented collars
- 8 Bullet gauges



## SP302

- 12 instrumented collars
- 8 Bullet gauges
- 12 Tie rods (End cage)



Courtesy of S. Mugnier EDMS #2711698

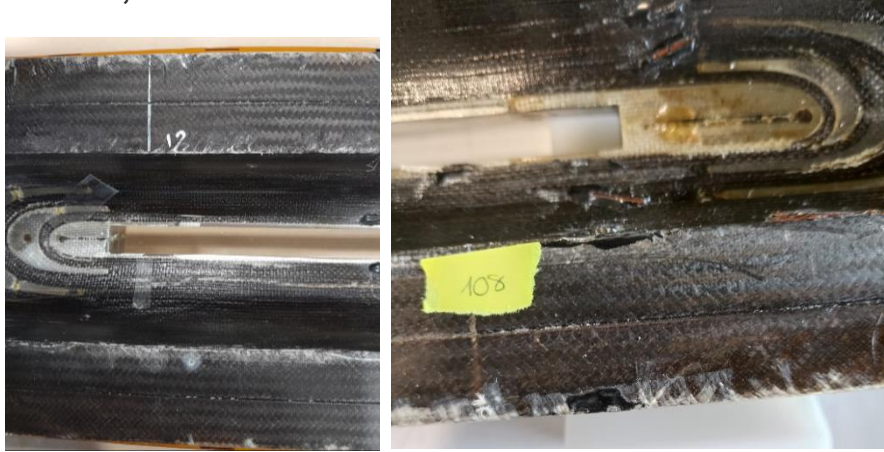


# Coils

Discussed in <https://indico.cern.ch/event/1326626/>

Coil 108

1<sup>st</sup> generation, RRP cable



Coil 212

2<sup>nd</sup> generation, PIT cable



212 MP left

Coil 214 – new

2<sup>nd</sup> generation, PIT cable



Coil 213

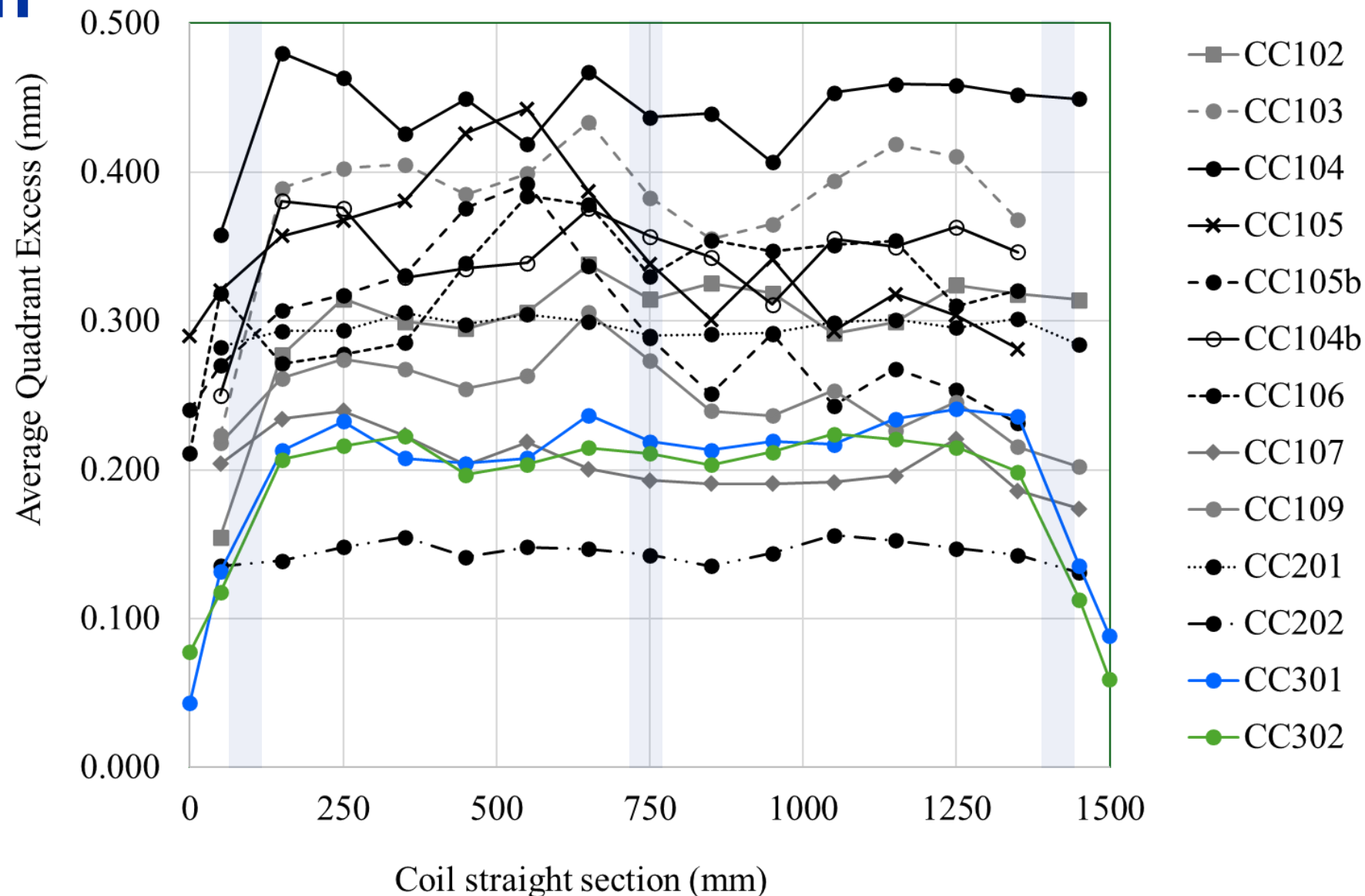
2<sup>nd</sup> generation, PIT cable



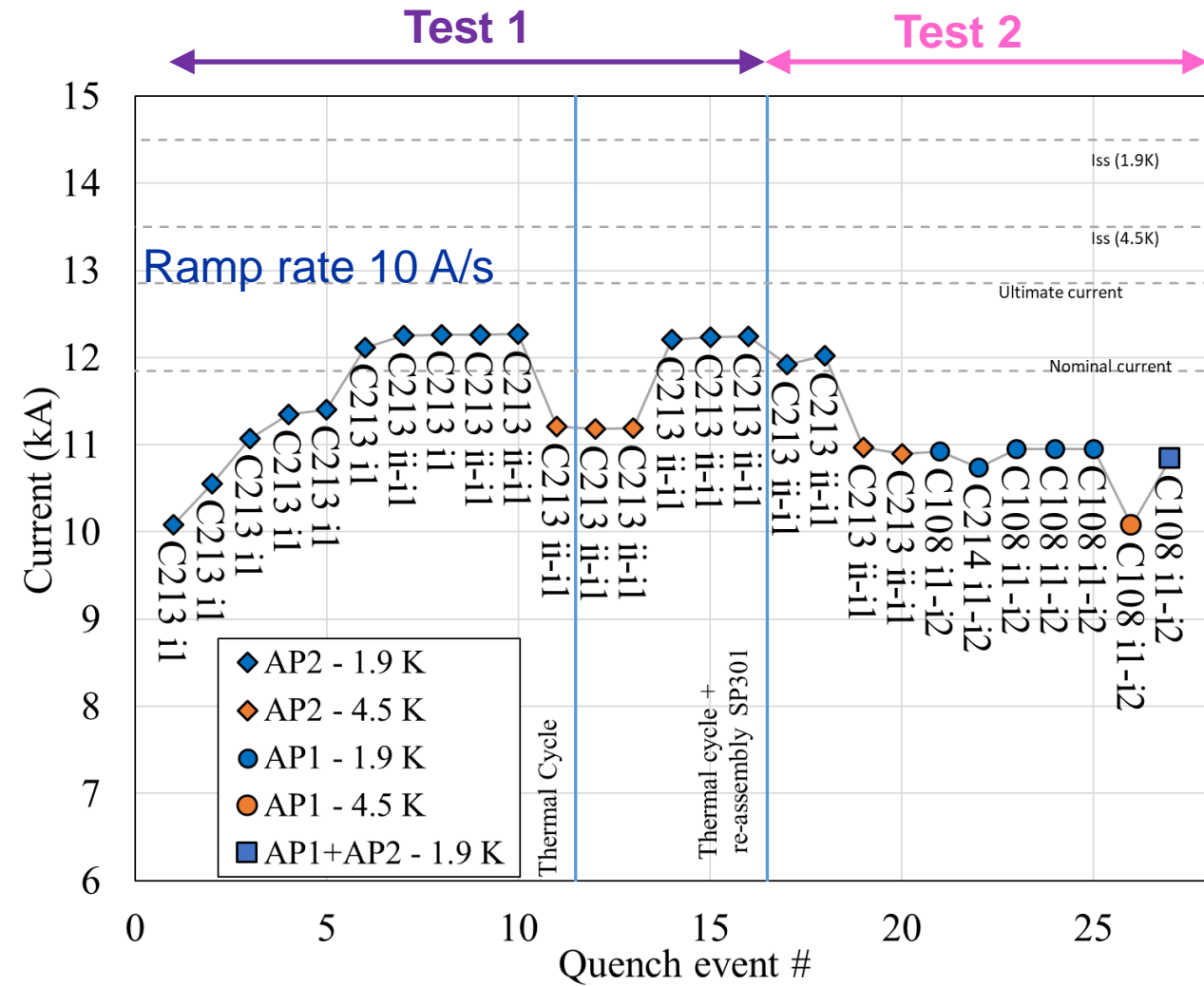
213 MP right

# Shimming plan

- **Excess reduction** in the last 150 mm until 75  $\mu\text{m}$  approximately.
- Measurements of the **virgin coil** used because the equivalent stiffness of the coil depends on the maximum stress previously seen by the coil mid-plane [3].
- Measurements reports: [108](#), [212](#), [213](#), [214](#).

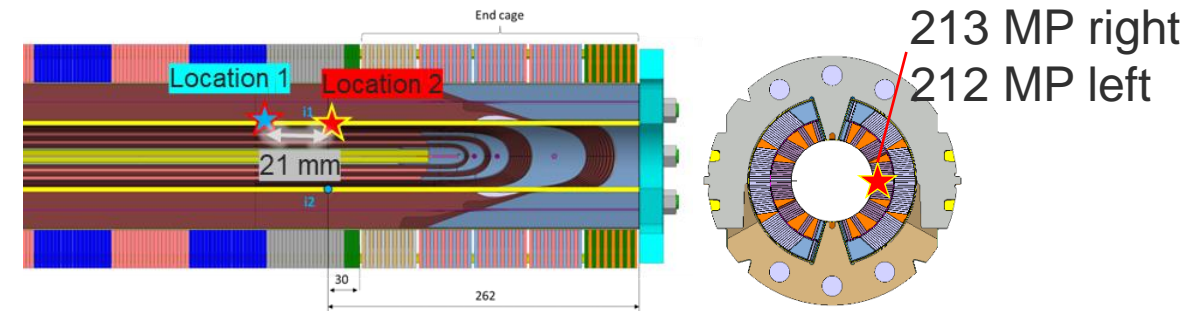


# 3. Cold test results



### Test 1:

- Powering of SP302: limit 12.2 kA at 1.9k, 500 A less than these coils in DP201 magnet [4]; location coil 213 NCS mid plane inner layer, close to the end cage location.
- No powering of SP301, HL-LHC NCR.



From <https://indico.cern.ch/event/1417760/> G. Willering

### Test 2:

- Powering of SP302: limit 12 kA at 1.9k, 200A less than in test 1; location coil 213 NCS mid plane inner layer, close to the end cage location.
- Powering of SP301: limit 10.9 kA at 1.9 K, coil 108 NCS inner layer first turn head. Coil 108 reached 13.2 kA at 1.9 K on its previous test in magnet DP101 [2].

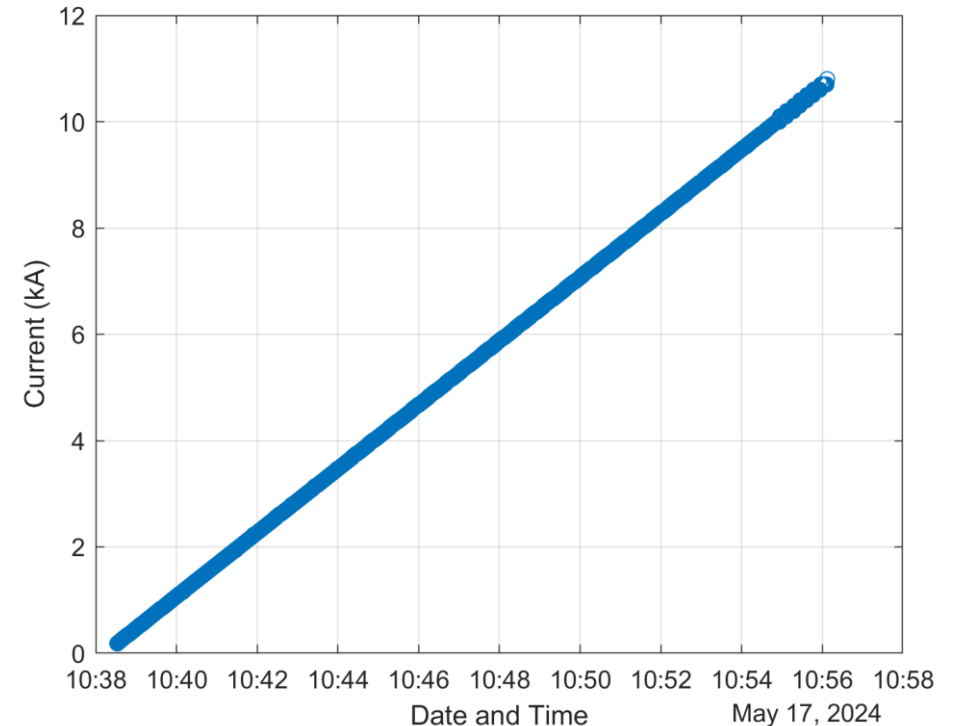
# 4. Mechanical measurements

# Some words

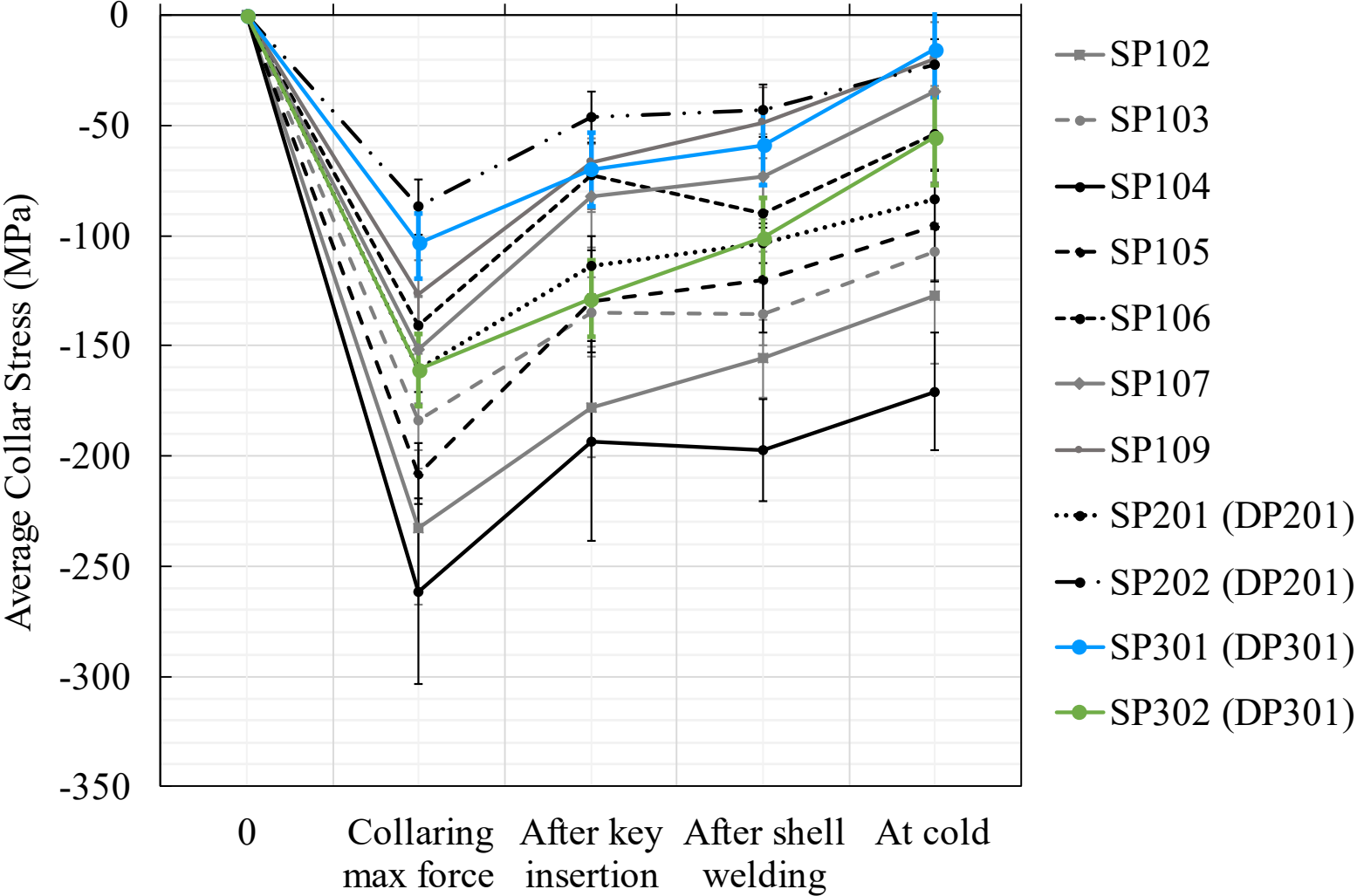
The 3D model [1]:

- Long magnet
- Symmetry
- Connection side
- Friction between coil and collars
- Collars and yoke are bulk but with modified properties to consider the longitudinal behaviour
- Collaring is not modelled. It directly applies to the coil the desired pre-stress
- Powering at nominal current 11.85 kA
- Roxie axial electromagnetic forces:  
 $F_z = 477 \text{ kN/collared coil} + \text{Volumetric forces}$   
calculated in Comsol.

Quench of both apertures for the mechanical measurements analysis 10.8 kA

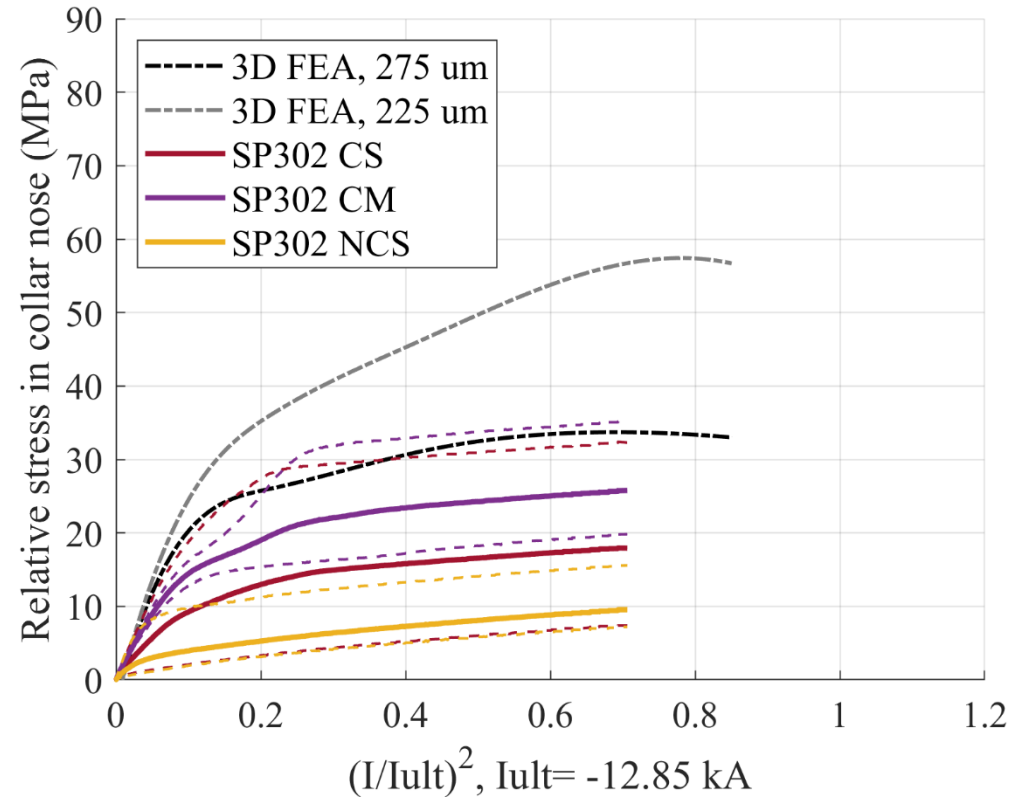
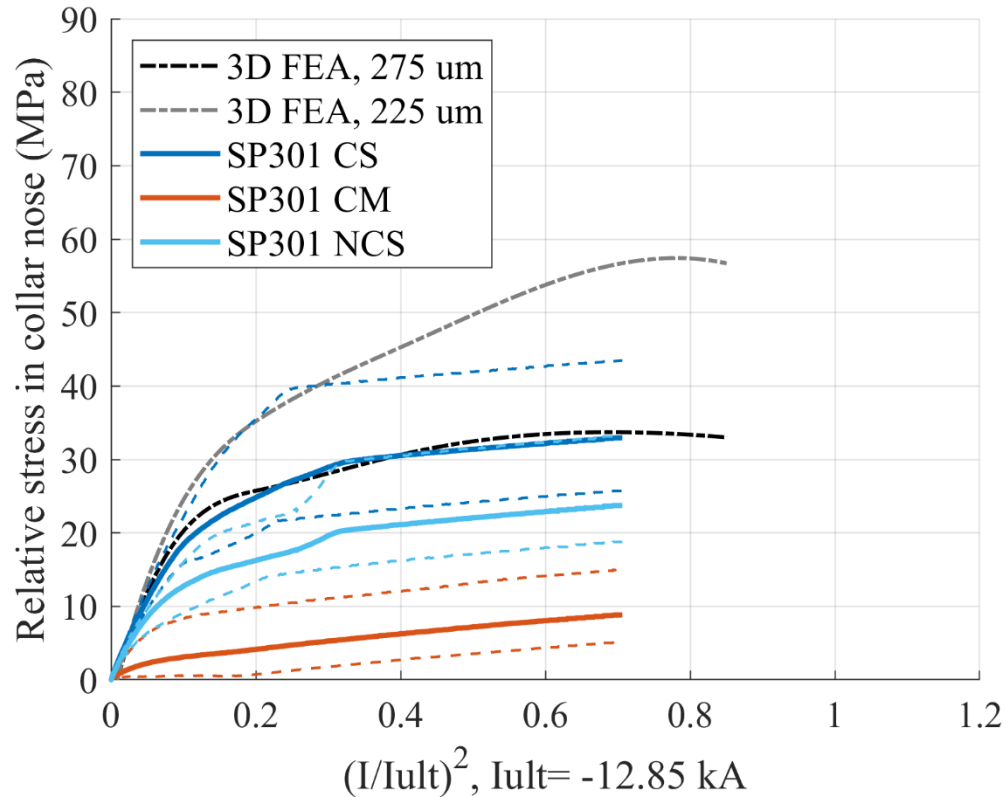


# Collar nose stress (1)



- The delta cool down in SP301 and SP302 (44 MPa) is bigger than the average observed in previous models (27 MPa) due to the larger thermal contraction of the stainless-steel pole (2.95 mm/m) compared to titanium (1.7 mm/m).
- This difference has been verified using a 2D model of a 1-in-1 magnet, which showed that the delta cool down for 200 um excess is 35 MPa for stainless steel pole, compared to 22 MPa in the titanium pole.

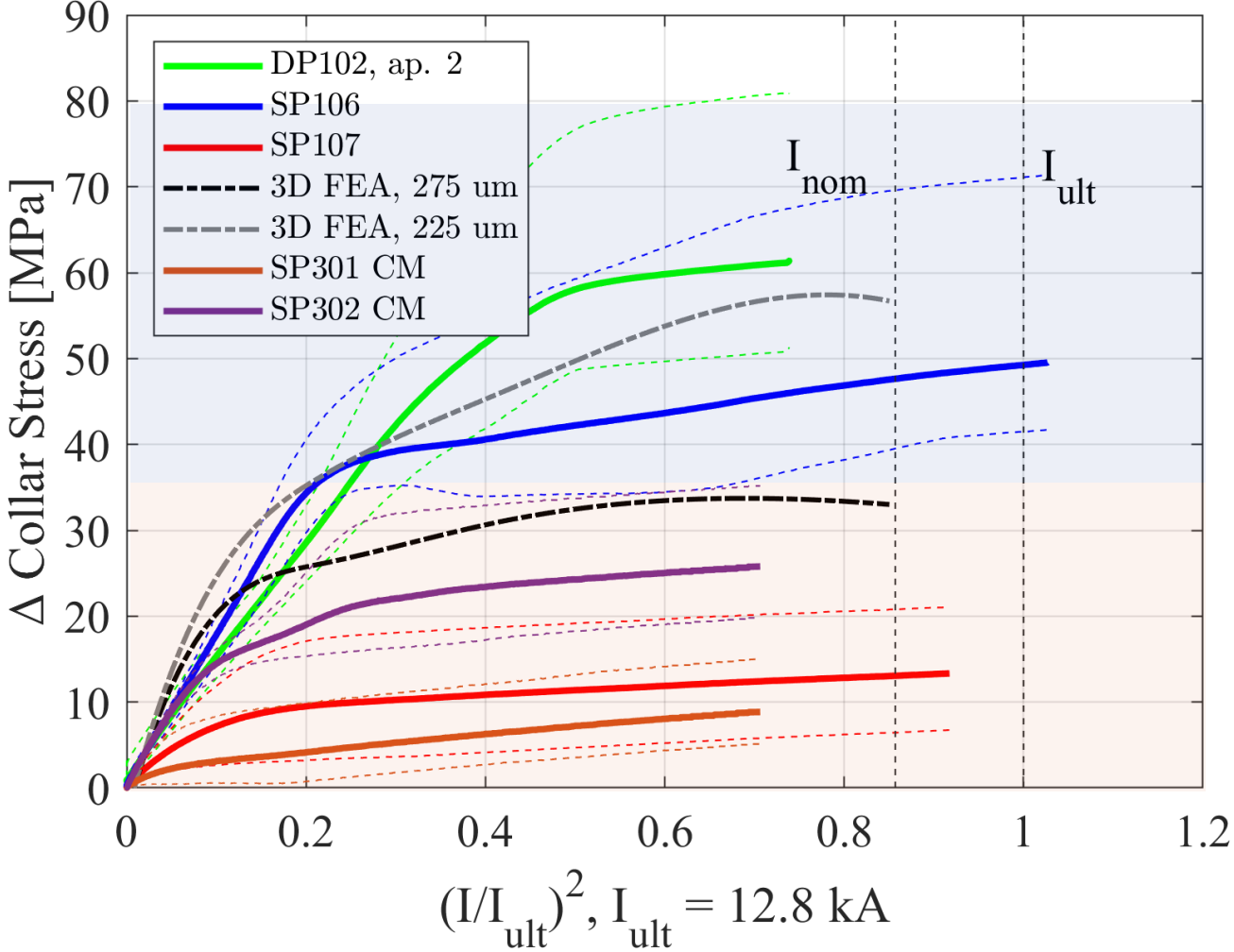
# Collar nose stress (2)



The continuous lines represent the average of the collars section, average of four collars. The dotted lines represent the maximum and minimum measured in the collars section. FEA lines in different longitudinal positions, different excess.



# Collar nose stress (3)



Zone excess  
0.3 mm/quadrant

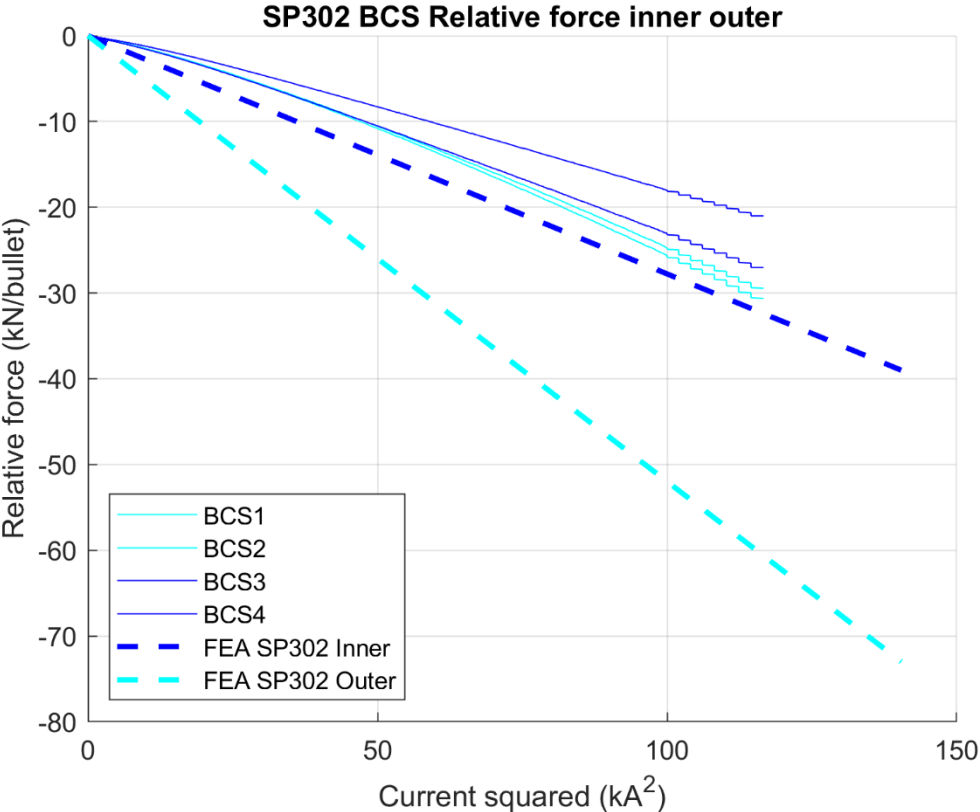
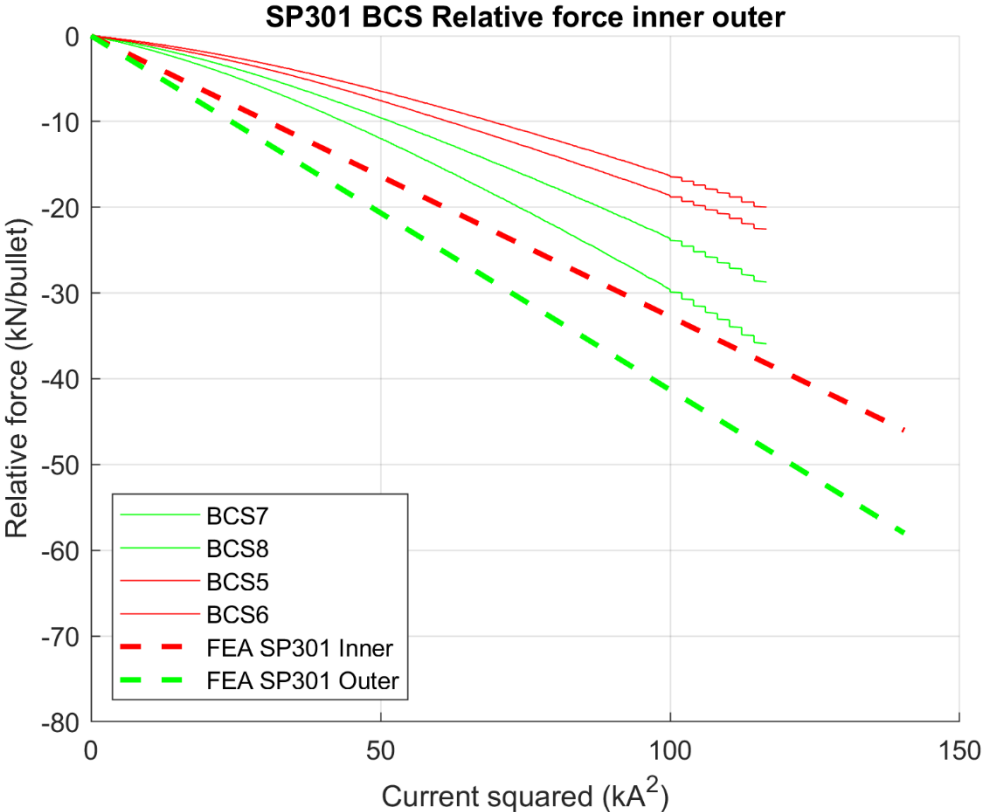
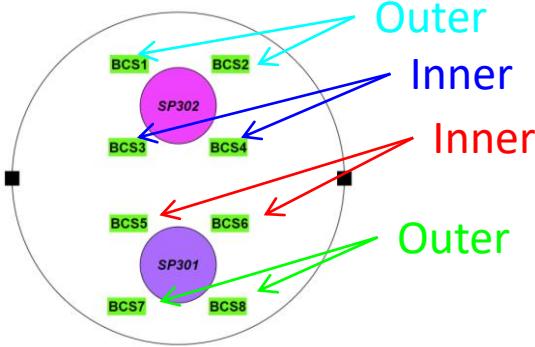
Zone excess  
0.2 mm/quadrant

# Magnet end plate bullets (1)



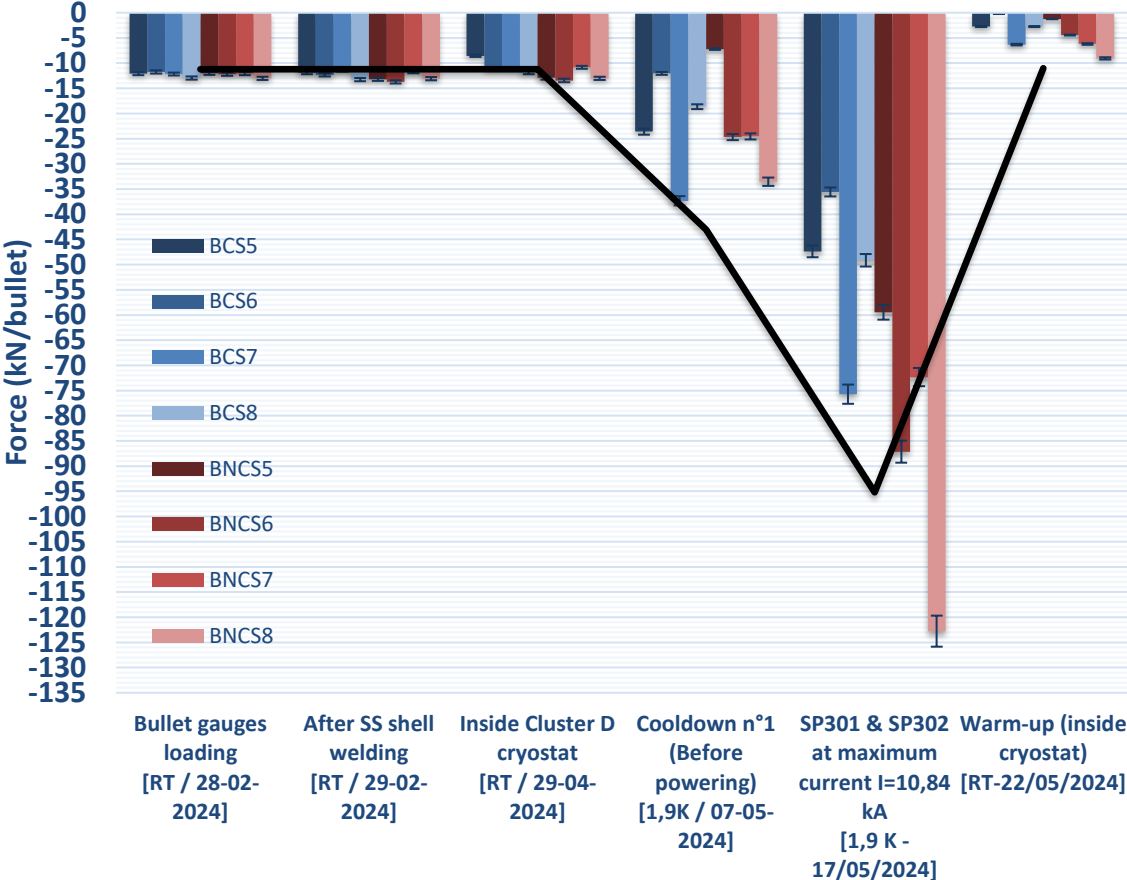
# Magnet end plate bullets (2)

Only connection side represented

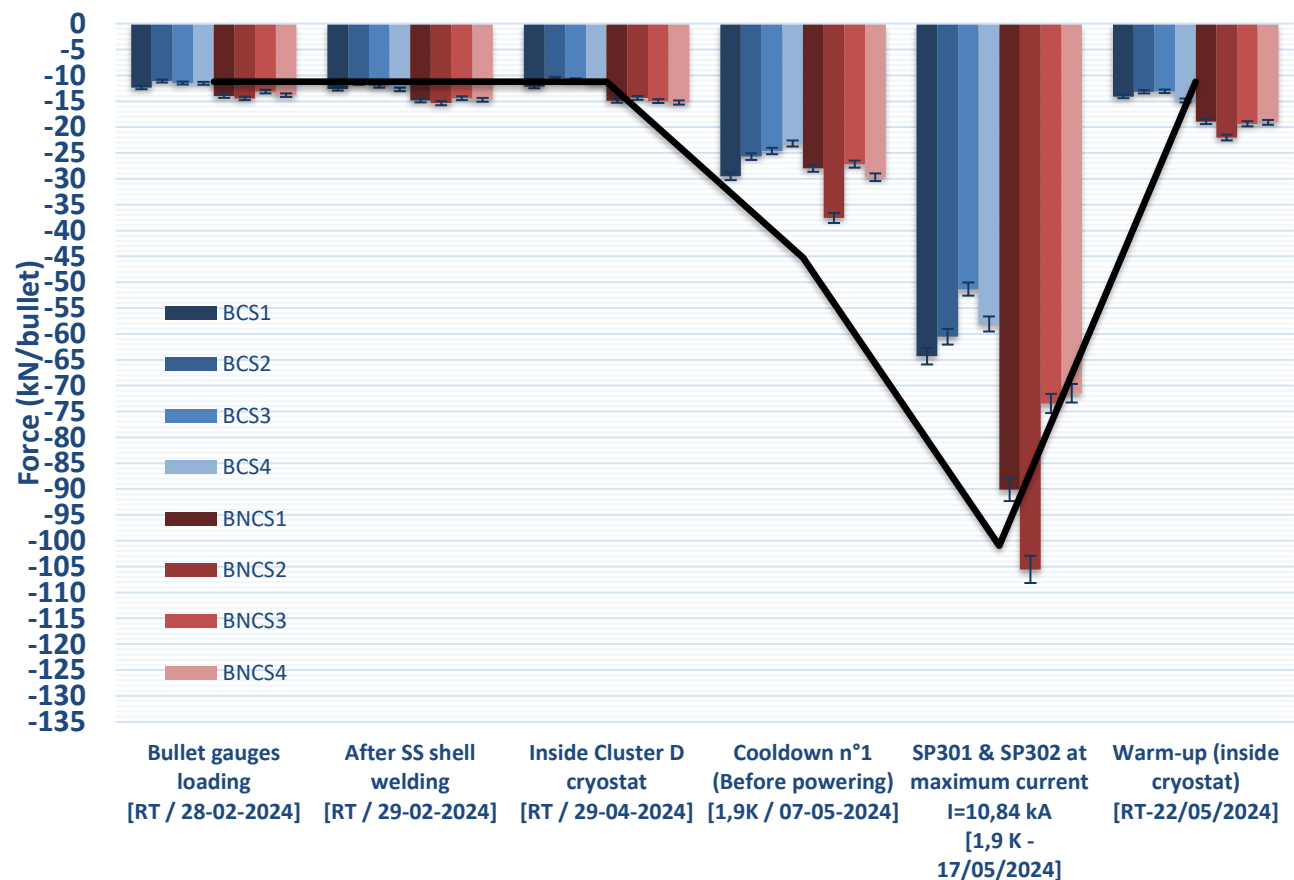


# Magnet end plate bullets (3)

### End Plates bullets SP301 - Longitudinal Force



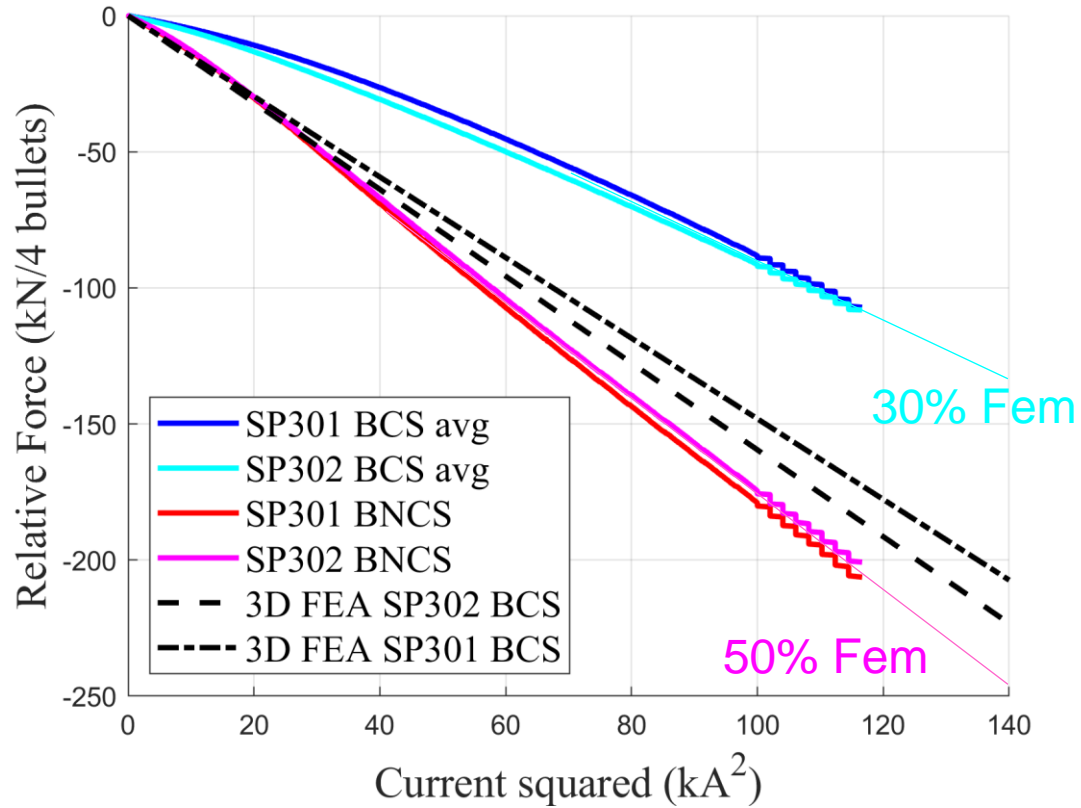
### End Plate bullets SP302 - Longitudinal Force



From EDMS #2711698 S. Mugnier



# Magnet end plate bullets (4)



- Higher slope in non connection side, consistent with previous double aperture models [2].
- This phenomenon is attributed to the length difference of both sides, resulting in increased frictional force dissipation on the connection side. These measurements are valuable for calibrating numerical models.
- The forces transmitted to the bullets are inversely proportional to the length of the side:

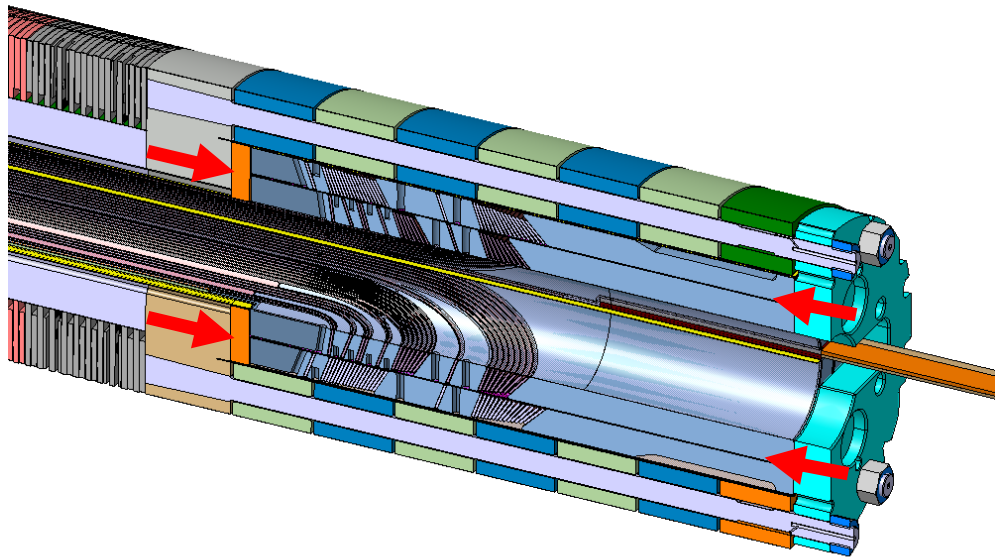
$$\frac{l_{headCS}}{l_{headNCS}} = 1.7$$

$$\frac{F_{em\_bulletsNCS}}{F_{em\_bulletsCS}} = 1.7$$

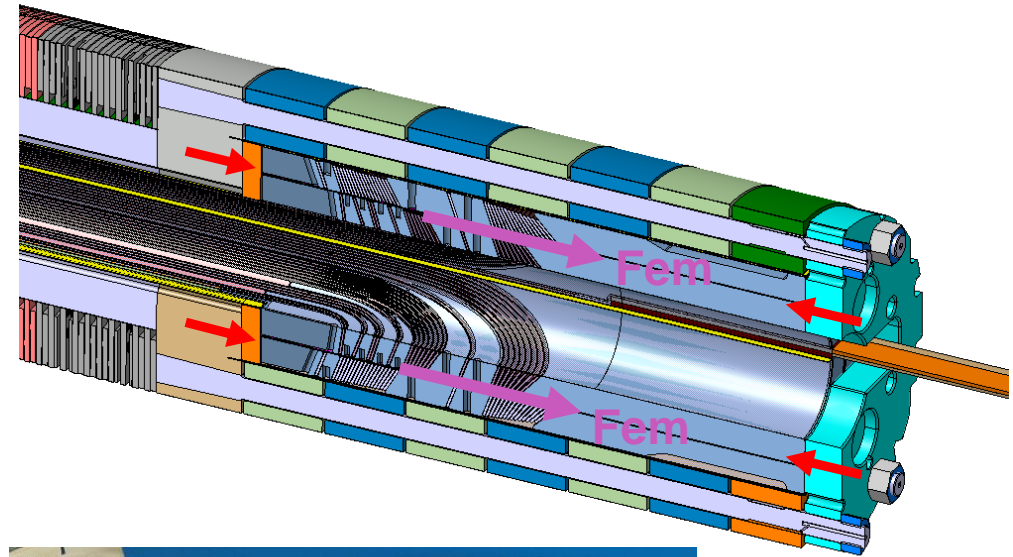
- The sum of the transferred forces to the bullets per aperture is the same but the spread is slightly larger in the aperture without end cage.

# End cage rods (1)

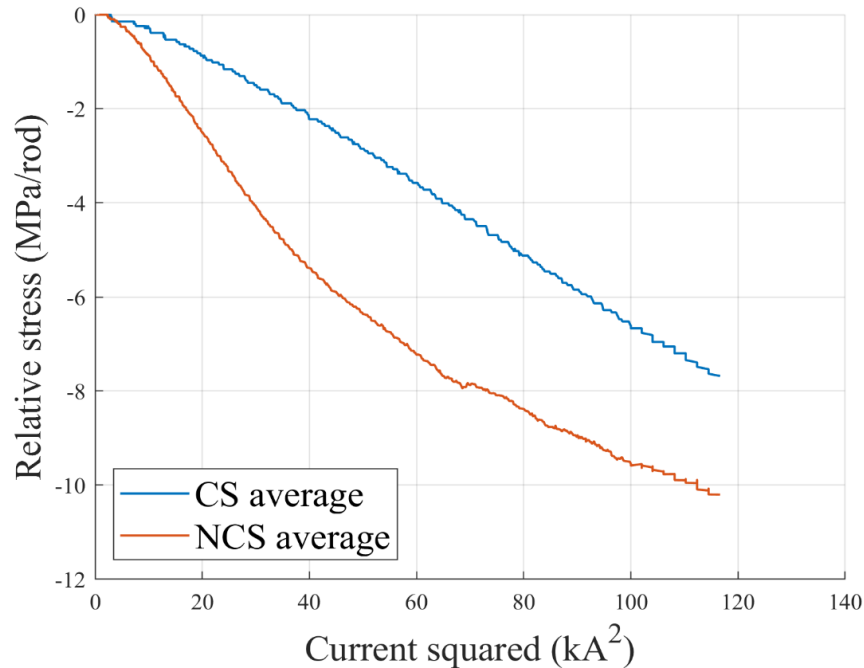
End cage activation – room temperature  
Force shared between coil inner and outer layer.  
Preload with 12% of the electromagnetic forces,  
29 kN/coil. Loading [report](#).



Energization – 1.9k



# End cage rods (2)



- No agreement between the 3D model and experimental measurements; the model shows an average delta powering of 52 MPa, almost 5 times larger.
- No linear behaviour of the non-connection side rods during powering.
- Unbalance in the rods stresses in connection side after cool down.
- The rods are always under tension, ensuring constant compaction of the coil head.

SP302 Rods train gauges (MPa)				3D FEA (MPa)		
	Loading	Cold	Powering	Loading	Cold	Powering
CS	88	81	71 (128,63,49,44)	115	100	48 (33,48,64)
NCS	66	52	37 (7,62,30,52,41,33)	-	-	-

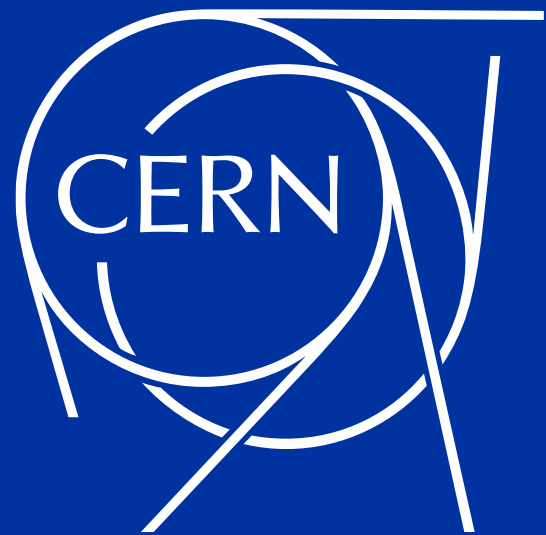
# 5. Conclusions

- Despite no alterations in the aperture SP302 between tests, the local damage increased (loss of 200 A in quench current) after thermal cycle and magnet re-assembly.
- In **SP302**, the quench appears near the end cage; however, it cannot be confirmed that this is due to the end cage, as the coils were damaged and repaired (increasing the mid-plane thickness) in this area.
- In **SP301**, the quench occurs at a very low current. Coil 108 seems to have significant damage in the inner layer NCS head.
- The effect of the material pole change is visible in the cool down reading of the **collar nose stresses**. The 3D model represents collar behaviour during powering.
- The factor of the electromagnetic forces transferred to the **bullets in CS and NCS** is inversely proportional to the length. The aperture with the end cage, SP302, shows a smaller spread of the transfer forces during cool down and powering due to the homogenization of axial loading by the end cage end plate.
- The **end cage rods** remain under tension, ensuring coil head compaction. However, performance limitations of the coils prevent definitive conclusions regarding potential enhancements in magnet performance.



# 6. References

- [1] C. Garion, M. Morrone, "Mitigation solutions on the 11 T magnet," CERN Internal technical note, Geneva, 2022.
- [2] S. Izquierdo et al., "Mechanical analysis of the Nb<sub>3</sub>Sn 11 T dipole short models for the High Luminosity Large Hadron Collider"
- [3] J. L. Rudeiros Fernandez "Characterization of the Mechanical Properties of Nb<sub>3</sub>Sn Coils" IEEE Transactions on applied superconductivity, vol. 29, no. 5, AUGUST 2019, Art. no. 8401205.
- [4] E. Gautheron *et al.*, "Pre-Load Studies on a 2-m Long Nb<sub>3</sub>Sn 11 T Model Magnet for the High Luminosity Upgrade of the LHC"

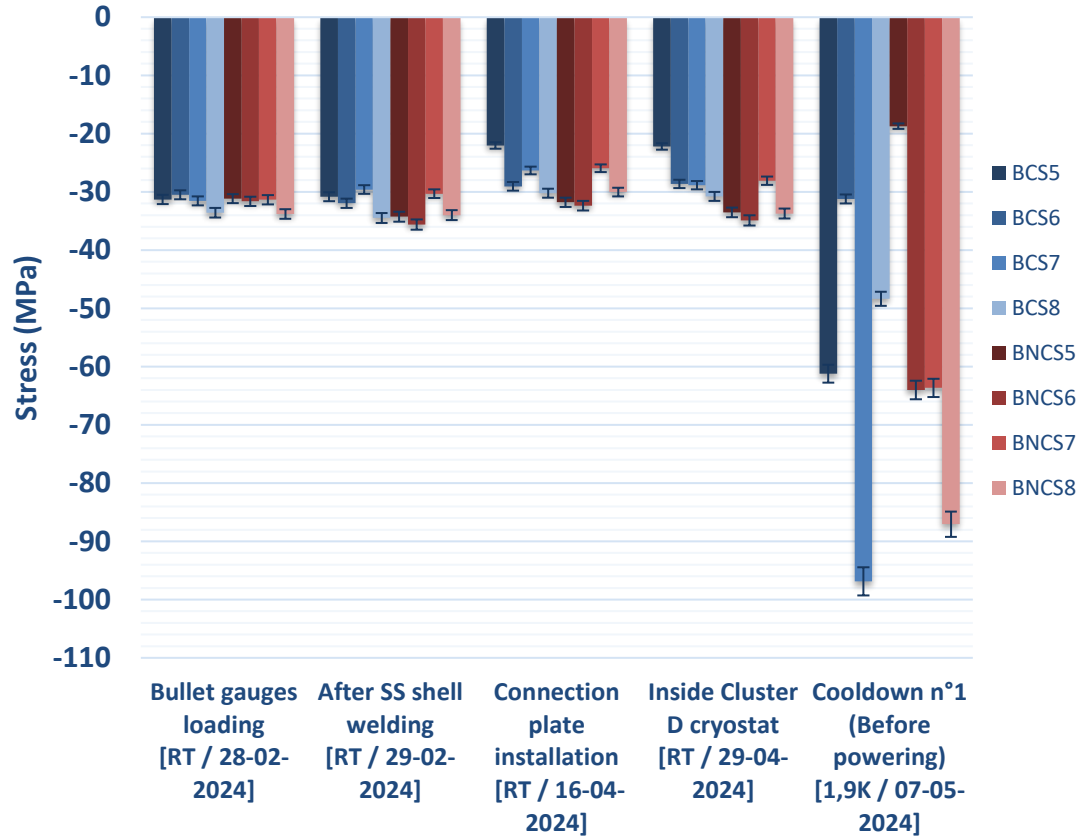


# Collaring parameters of the reused coils for the magnet MBHDP301b

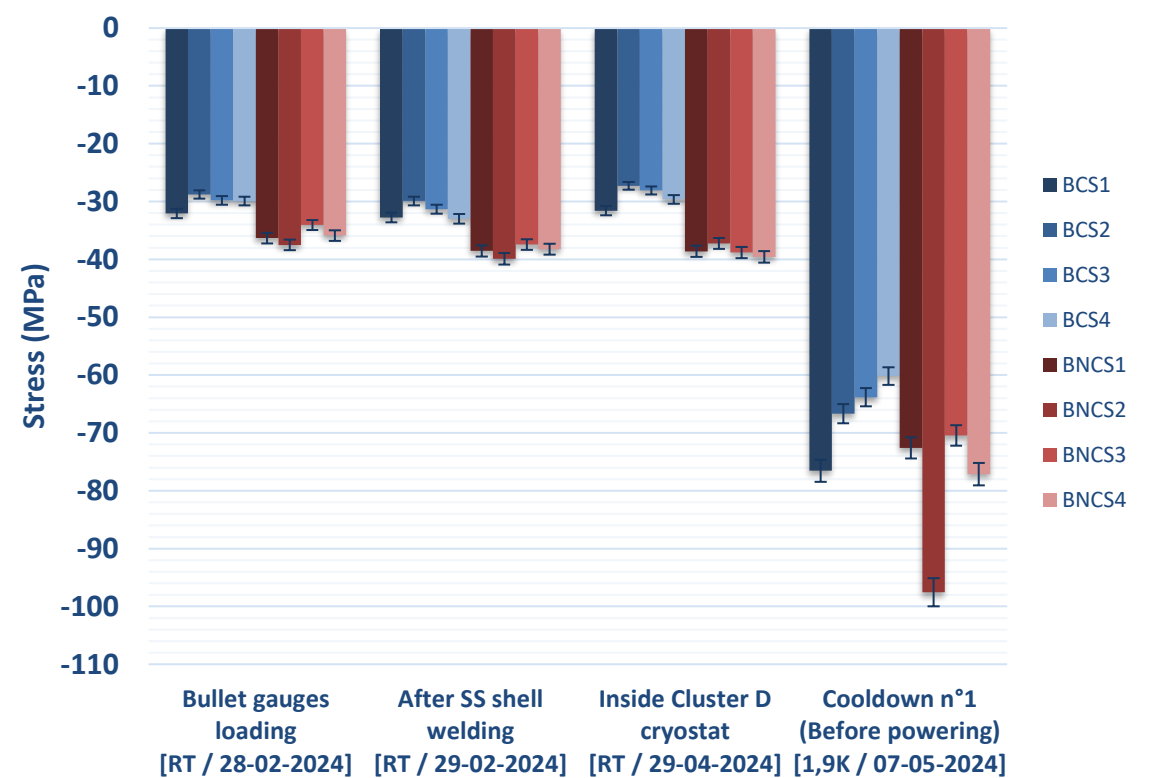
Parameter	Unit	Collared coil									
		CC102		CC999		CC202		CC301		CC302	
		106	108	106	108	212	213	108	214	212	213
Collaring											
Nominal collaring cavity	mm	70	70	70	70	70	70	70	70	70	70
Stoppers height, including shims	mm	70.1	69.85	69.85	69.85	69.85	69.85	69.85	69.85	69.85	69.85
Key clearance	um	-100	150	150	150	150	150	150	150	150	150
Collaring force	MN	34.0	8.5	6.0	5.4	6.6	6.6	5.4	6.0	8.5	34.0
Collar nose stress at max collaring force	MPa	-227	-	-86	-103	-161	-161	-103	-86	-	-227
Collar nose stress after key insertion	MPa	-186	-	-46	-65	-130	-130	-65	-46	-	-186

# Bullet spread values during cool down

MBHDP301b - End Plates bullets MBHSP301 -  
Longitudinal Stress

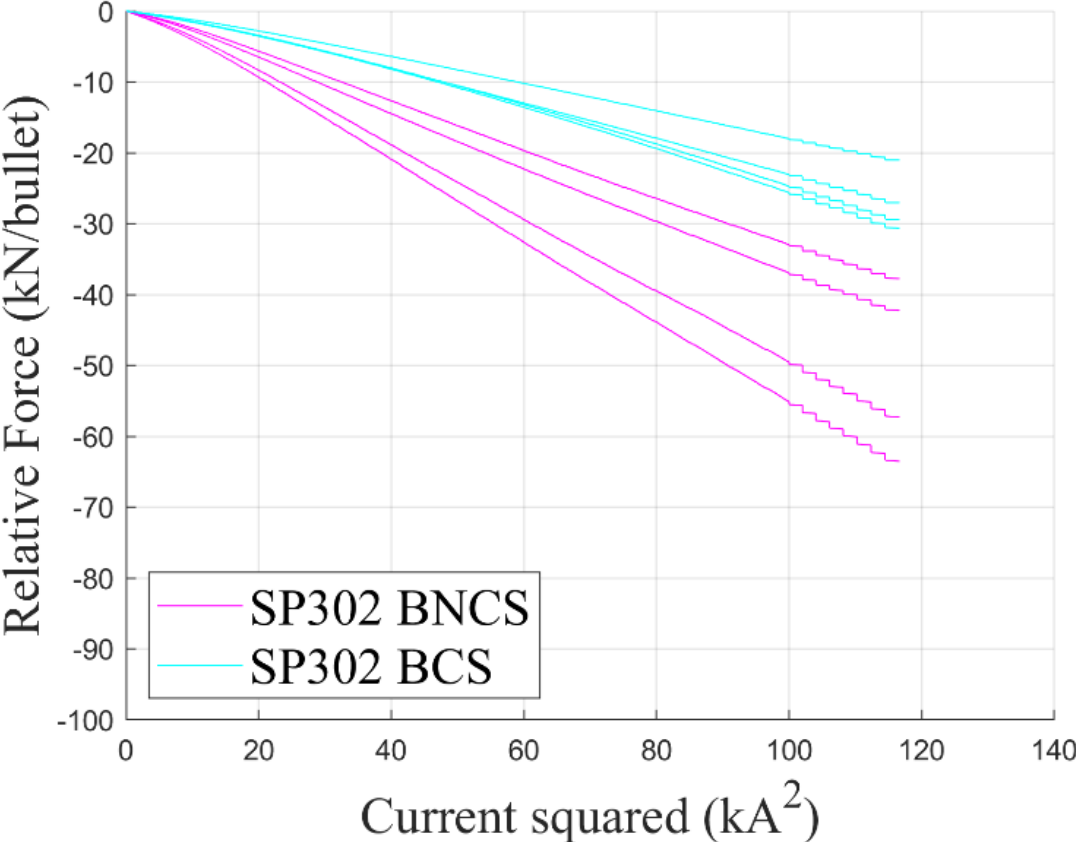
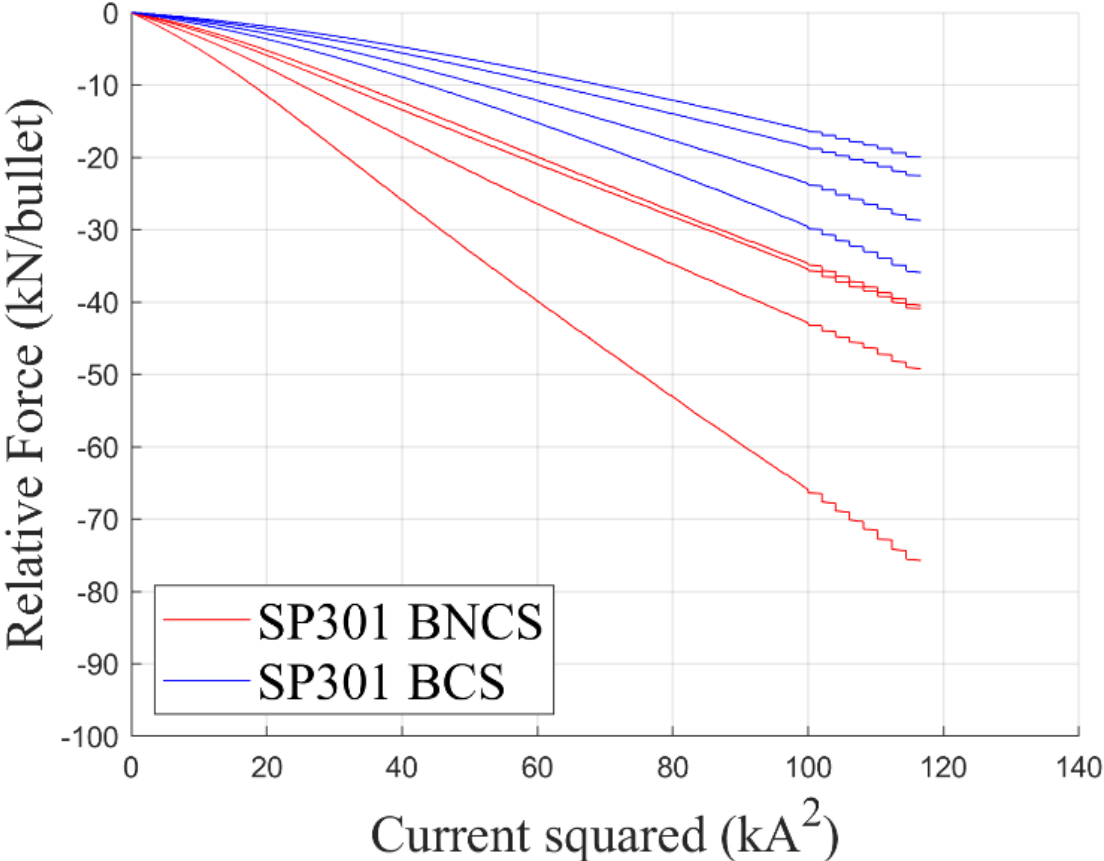


MBHDP301b - End Plates bullets MBHSP302 -  
Longitudinal Stress

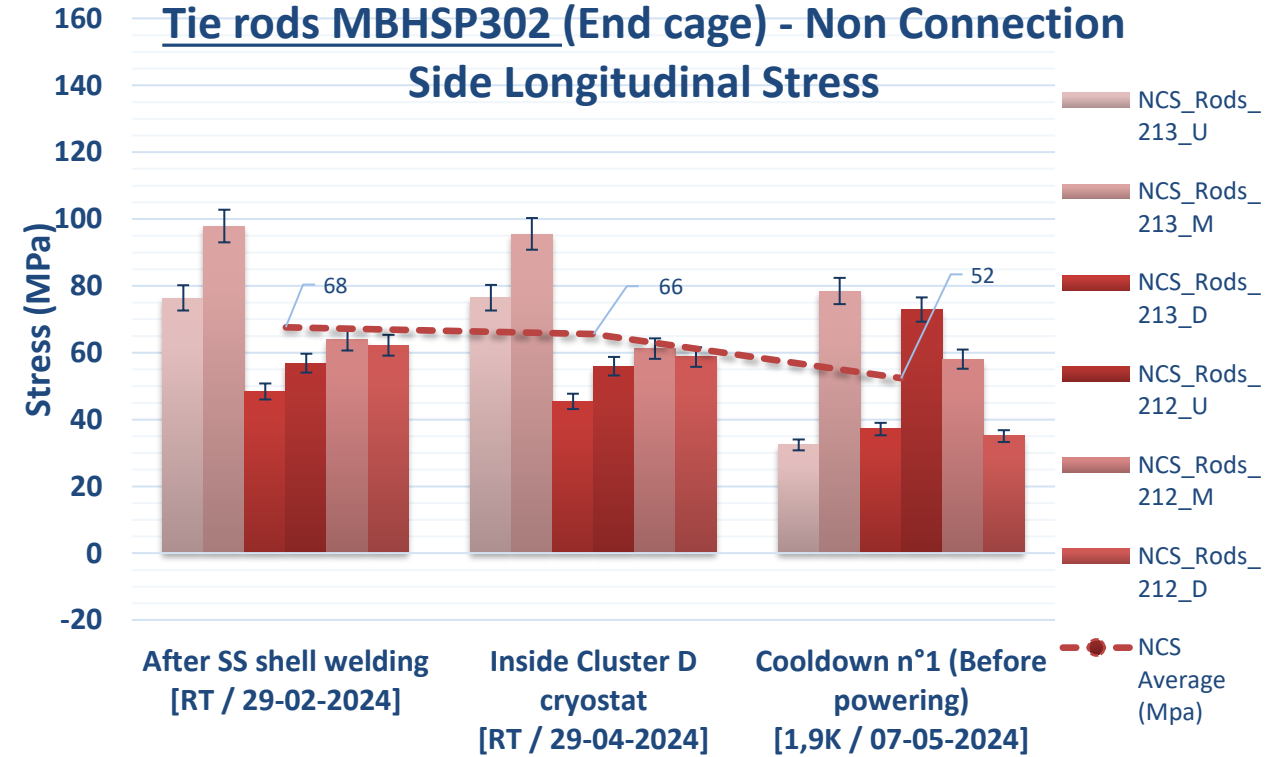
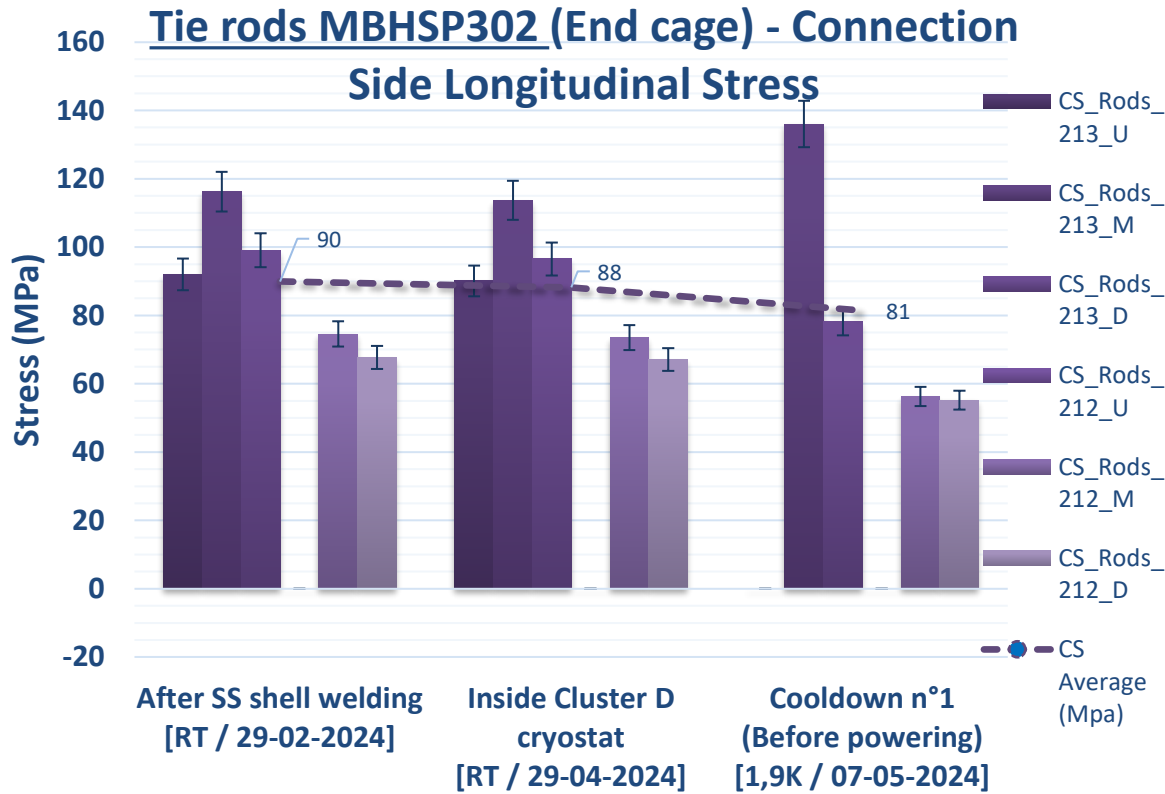


Courtesy of S. Mugnier EDMS #2711698

# Bullets spread values during powering



# End cage rods from loading to cool down



Courtesy of S. Mugnier EDMS #2711698

# Analytical calculation of coil head elongation

$$\Delta L = \frac{F_{EM}}{K_{coil}}$$

$$\Delta L = \frac{F_{EM}}{K_{rods} + K_{coils}}$$

Parameter	Unit	CS	NCS
e.m Force, Nominal Current	MN		0.478
Coil stiffness	MN/mm	3.7	6.3
Rod stiffness	MN/mm	0.5	0.1
Coil elongation without rods, no friction	um	65	38
Coil elongation with rods, no friction	um	46	35

$$K_{coil} = \sum \frac{E_i A_i}{l_i} = \frac{E_{coil} A_{coil}}{l_{coil}} + \frac{E_{G11} A_{G11}}{l_{G11}} = A \left[ \frac{E_{coil}}{l_{coil}} + \frac{E_{G11}}{l_{G11}} \right]$$

$$K_{rods} = \frac{EA}{l}$$